Coupled Lateral and Longitudinal Control for Vehicle Platoons on Curved Roads

Bocheng Ma, Yang Zhu* and Hongye Su
College of Control Science and Engineering, Zhejiang University, Hangzhou, Zhejiang, China

Keywords: Vehicle Platoon, Longitudinal and Lateral Coupling, Frenet Coordinate System, Distributed Model Predictive Control.

Abstract: This paper presents a longitudinal and lateral coupling control model for platoons on roads with varying curvature. The model integrates a 3-DOF vehicle dynamic model with lateral distance errors using the Frenet coordinate system and employs a distributed predictive controller. This approach ensures that vehicles within the platoon maintain ideal inter-vehicle distances, follow the leader's speed, and remain within their lanes, effectively addressing the "cutting-corner" issue. Joint simulations using Carsim and Matlab demonstrate that the model effectively maintains ideal inter-vehicle distances and tracks the leader's speed, even with changes in the leader's velocity.

1 INTRODUCTION

As transportation technology advances, the growing demand for travel has led to numerous issues, including increased traffic accidents, severe congestion, and worsening environmental pollution. Within autonomous driving technology, platoon control—enhanced by developments in V2X communication—has gained significant research interest due to its advantages in improving safety(Dai et al., 2022), alleviating congestion(Zeng et al., 2023), and boosting traffic efficiency(Ma et al., 2021).

The PATH project has made groundbreaking contributions to platoon control, addressing numerous associated challenges (Rajamani et al., 2000). A framework for platoon modeling introduced by (Li et al., 2017; Basiri et al., 2020) includes four key components: Node Dynamics, Information Flow Network, Distributed Controller, and Formation Geometry, which has advanced the field further. Distributed Model Predictive Control (DMPC) is widely widely applied in multi-agent cooperative control(He et al., 2024), especially in platoon control(Negenborn and Maestre, 2014; Zheng et al., 2017) for its ability to reduce computational load and communication delays in large-scale platoons while managing complex constraints effectively.

Most existing platoon control systems have concentrated on straight roads, focusing primarily on longitudinal control (Kwon and Chwa, 2014; Dunbar and Caveney, 2012), and have often overlooked lateral dynamics. Given the practical challenges of platoon operation on curved roads, addressing control in such conditions is of considerable importance. The cutting-corner problem on curved roads remains a significant challenge (Zhao et al., 2022). The approach proposed by (Bayuwindra et al., 2020), which utilizes an extended look-ahead strategy, addresses this issue without requiring road information, relying instead on vehicle data. However, incorporating road information into controllers can enhance performance in more complex scenarios. Many control strategies simplify design by separating lateral and longitudinal control (Wu et al., 2022; Kianfar et al., 2014). The lateral and longitudinal coupled platoon control model offers improved precision and following performance, making it a valuable and challenging area for research. The Frenet coordinate system is frequently employed in controllers that integrate road information, as it simplifies path tracking and effectively manages curved road data (Zuo et al., 2024).

This paper presents a lateral and longitudinal coupled platoon control model, integrating the 3-D0F dynamic vehicle model with lateral distance errors in the Frenet coordinate system (Wei et al., 2019). This integration facilitates optimal performance for platoons on curved roads.

*Corresponding author.

Ma, B., Zhu, Y. and Su, H.
Coupled Lateral and Longitudinal Control for Vehicle Platoons on Curved Roads.
DOI: 10.5220/0013131500003941
In *Proceedings of the 11th International Conference on Vehicle Technology and Intelligent Transport Systems (VEHITS 2025)*, pages 286-293
ISBN: 978-989-758-745-0; ISSN: 2184-495X

2 VEHICLE PLATOON MODEL

In this paper, as shown in Figure 1, a platoon of vehicles on the curved road is presented, which consists of a leader vehicle and several following vehicles. The leader vehicle is denoted as 0, and the following vehicles are denoted as 1 to N, respectively.

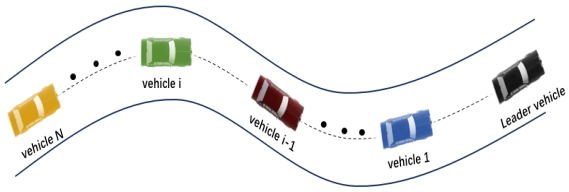

Figure 1: Vehicle platoon on the curved road.

2.1 Vehicles Dynamics Model

Since the vehicle platoon in this paper needs to travel on roads with varying curvature, both lateral and longitudinal motion control is required. Therefore, as shown in Figure 2, we introduce a 3-DOF dynamic bicycle model of the vehicle

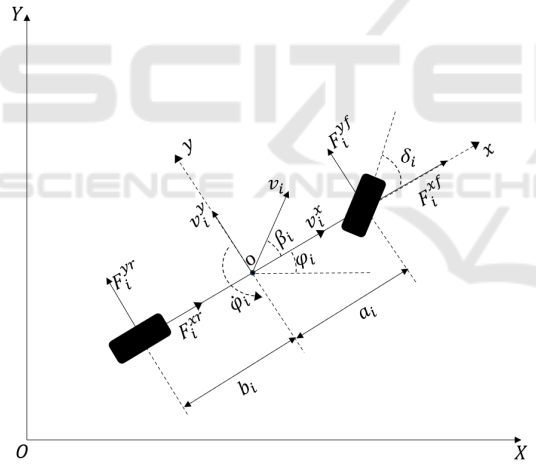

Figure 2: 3-DOF dynamic bicycle model of the vehicle.

In Figure 2, X, O, and Y represent the Earth coordinate system, while x, o, and y represent the vehicle body coordinate system. Based on (Feng et al., 2024), set $u_i^{\mathrm{a}} = \dot{v}_i^{\mathrm{x}} = v_i^{\mathrm{y}}\dot{\varphi}_i + \frac{1}{m_i}F_i^{\mathrm{x}}$, we propose a new vehicles dynamics model which can be expressed as:

$$\begin{cases} \dot{v}_i^{\mathrm{x}} = u_i^{\mathrm{a}} \\ \dot{v}_i^{\mathrm{y}} = -v_i^{\mathrm{x}}\dot{\varphi}_i + \frac{1}{m_i}\left(-\frac{(C_i^{\mathrm{f}}+C_i^{\mathrm{r}})v_i^{\mathrm{y}}}{v_i^{\mathrm{x}}} - \frac{(C_i^{\mathrm{f}}a_i - C_i^{\mathrm{r}}b_i)\dot{\varphi}_i}{v_i^{\mathrm{x}}} + C_i^{\mathrm{f}}\delta_i\right) \\ \ddot{\varphi}_i = \frac{1}{I_i^z}\left(-\frac{(C_i^{\mathrm{f}}a_i - C_i^{\mathrm{r}}b_i)v_i^{\mathrm{y}}}{v_i^{\mathrm{x}}} - \frac{(C_i^{\mathrm{f}}a_i^2 + C_i^{\mathrm{r}}b_i^2)\dot{\varphi}_i}{v_i^{\mathrm{x}}} + C_i^{\mathrm{f}}a_i\delta_i\right) \end{cases} \quad (1)$$

The subscript i denotes the i-th vehicle, where $i \in \{1,2,\ldots,N\}$. The mass of the i-th vehicle is denoted by m_i. The longitudinal and lateral velocities of the i-th vehicle are represented by v_i^{x} and v_i^{y}, respectively. The longitudinal forces on the front and rear tires are denoted by F_i^{xf} and F_i^{xr}, respectively, while the lateral forces on these tires are denoted by F_i^{yf} and F_i^{yr}. The moment of inertia of the i-th vehicle about the z-axis is represented by I_i^z. The distances from the front and rear axles to the center of mass of the i-th vehicle are denoted by a_i and b_i, respectively. The yaw rate of the i-th vehicle is given by $\dot{\varphi}_i$.

C_i^{f} and C_i^{r} represent the cornering stiffness of the front and rear wheels of the vehicle i, respectively. δ_i is the steering angle of the front tires of the i-th vehicle. u_i^{a} denotes the acceleration of the i-th vehicle.

2.2 Longitudinal and Lateral Error Model

Assuming the speed v_0 and position s_0 of the leading vehicle are *a priori* known, the goal of the following vehicles is to track the speed of the leading vehicle while maintaining a desired inter-vehicle distance. In this paper, the commonly used constant distance policy is adopted.

For each following vehicle i, $i \in \{1,2,\ldots,N\}$, let its position be defined as s_i. The position error is described as:

$$e_i^{\mathrm{p}} = s_0 - s_i - i \cdot d_{\mathrm{des}} \quad (2)$$

where d_{des} represents the desired inter-vehicle distance, which is a constant.

As shown in Figure 3, the lateral error l_i is defined in the Frenet coordinate system as the distance between the vehicle's center of mass and its projection onto the reference line.

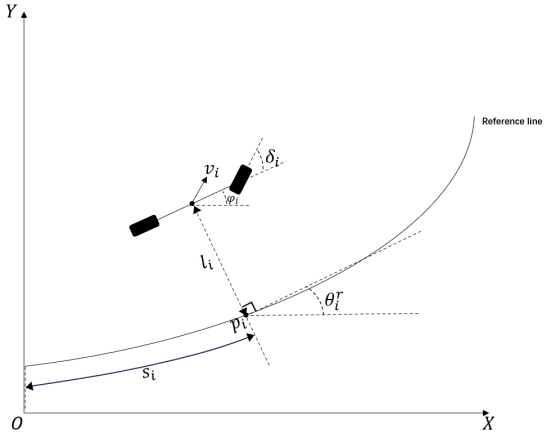

Figure 3: Lateral error in the Frenet coordinate system.

Here, p_i is the projection of the center of mass of vehicle i onto the reference line; v_i is the velocity of the center of mass of vehicle i; φ_i is the yaw angle of vehicle i; and θ_i^{r} is the angle between the tangent to the reference line at p_i and the X-axis. The derivative of l_i with respect to time t is as follows:

$$\dot{l}_i = v_i^{\mathrm{y}} \cos(\varphi_i - \theta_i^{\mathrm{r}}) + v_i^{\mathrm{x}} \sin(\varphi_i - \theta_i^{\mathrm{r}}) \tag{3}$$

2.3 Longitudinal and Lateral Coupled Model

By combining equations (1), (2), and (3), we obtain the longitudinal and lateral coupling model for vehicle i:

$$\begin{cases} \dot{v}_i^{\mathrm{x}} = u_i^{\mathrm{a}} \\ \dot{v}_i^{\mathrm{y}} = -v_i^{\mathrm{x}}\dot{\varphi}_i + \frac{1}{m_i}\left(-\frac{(C_i^{\mathrm{f}}+C_i^{\mathrm{r}})v_i^{\mathrm{y}}}{v_i^{\mathrm{x}}} - \frac{(C_i^{\mathrm{f}}a_i - C_i^{\mathrm{r}}b_i)\dot{\varphi}_i}{v_i^{\mathrm{x}}} + C_i^{\mathrm{f}}\delta_i\right) \\ \ddot{\varphi}_i = \frac{1}{I_i^z}\left(-\frac{(C_i^{\mathrm{f}}a_i - C_i^{\mathrm{r}}b_i)}{v_i^{\mathrm{x}}} - \frac{(C_i^{\mathrm{f}}a_i^2 + C_i^{\mathrm{r}}b_i^2)\dot{\varphi}_i}{v_i^{\mathrm{x}}} + C_i^{\mathrm{f}}a_i\delta_i\right) \\ \dot{\varphi}_i = \dot{\varphi}_i \\ \dot{e}_i^{\mathrm{p}} = v_0 - v_i \\ \dot{l}_i = v_i^{\mathrm{y}}\cos(\varphi_i - \theta_i^{\mathrm{r}}) + v_i^{\mathrm{x}}\sin(\varphi_i - \theta_i^{\mathrm{r}}) \end{cases} \tag{4}$$

Discretize the system and define the state variables as follows:

$$X_i(k) = [v_i^{\mathrm{x}}(k)\ v_i^{\mathrm{y}}(k)\ \dot{\varphi}_i(k)\ \varphi_i(k)\ e_i^{\mathrm{p}}(k)\ l_i(k)]^T \tag{5}$$

The control inputs are the acceleration and the front wheel steering angle, defined as:

$$U_i(k) = [u_i^{\mathrm{a}}(k)\ \delta_i(k)]^T \tag{6}$$

The output is given by:

$$y_i(k) = [v_i^{\mathrm{x}}(k)\ e_i^{\mathrm{p}}(k)]^T \tag{7}$$

Using the Euler forward difference method, the discrete nonlinear model is given by:

$$\begin{cases} X_i(k+1) = \phi_i\big(X_i(k), U_i(k)\big) \\ y_i(k) = \gamma X_i(k) \end{cases} \tag{8}$$

$$\gamma = \begin{bmatrix} 1 & 0 & 0 & 0 & 0 & 0 \\ 0 & 0 & 0 & 0 & 1 & 0 \end{bmatrix}$$

where γ is the matrix defined above. The function $\phi_i\big(X_i(k), U_i(k)\big)$ is specified in equation (11), and T_{s} represents the discrete time interval.

3 DISTRIBUTED MODEL PREDICTIVE CONTROL

This section introduces the design of a Distributed Model Predictive Control (DMPC). Vehicles exchange and receive information based on the communication topology. Each vehicle transmits its own state and the received information to its upper-level DMPC controller, which then optimizes to compute the optimal control inputs. The DMPC controller adjusts the state of each vehicle to ensure coordinated behavior of the platoon.

3.1 Communication Topology

The design of the communication topology plays a crucial role in the formulation of the cost function in DMPC. The communication topology of the vehicle fleet can be represented by a directed graph $\mathbb{G} = \{\mathbb{V}, \mathbb{E}\}$, where $\mathbb{V} = \{0, 1, 2, \ldots, N\}$ is the set of vehicles, and $\mathbb{E} \subseteq \mathbb{V} \times \mathbb{V}$ is the set of edges that connect vehicles, and then define an N-order real-valued adjacency matrix $\mathcal{A} = [a_{ij}] \in \mathbb{R}^{N\times N}$, which is used to represent the communication relationship between any two vehicles

$$\mathcal{A} = [a_{ij}] = \begin{cases} a_{ij} = 1, & \text{if } \{j,i\} \in \mathbb{E} \\ a_{ij} = 0, & \text{if } \{j,i\} \notin \mathbb{E} \end{cases} \tag{10}$$

where $i, j \in \mathbb{V}$ and $\{j,i\} \in \mathbb{E}$ indicate a directed edge from j to i, meaning that information from vehicle j can be transmitted to vehicle i. We define $\mathbb{N}_i = \{j \mid a_{ij} = 1, j \in \{1,2,\ldots,N\}\}$ as the neighbor set of vehicle i, which implies that vehicle i can receive information from any vehicle $j \in \mathbb{N}_i$. Similarly, we define $\mathbb{O}_i = \{j \mid a_{ji} = 1, j \in \{1,2,\ldots,N\}\}$, representing the set of vehicles to which vehicle i can transmit information. In this paper, we adopt the commonly used predecessor-leader following (PLF) topology, as illustrated in Figure 4.

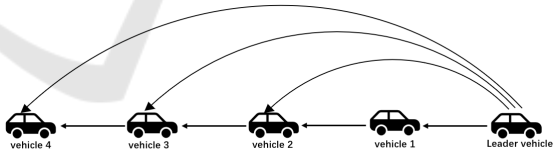

Figure 4: Predecessor-leader following (PLF) topology.

3.2 Controller Design

DMPC transforms the global problem into a local problem for each vehicle, where all vehicles simultaneously solve their own optimization problems.

Assume that the lead vehicle is not controlled and always follows the ideal trajectory. Then, according to equation (7), we define the reference values $X_{i,\mathrm{des}}(k)$ for the follower vehicles in the platoon:

$$\begin{aligned} &X_{i,\mathrm{des}}(k) = \\ &[v_{i,\mathrm{des}}^{\mathrm{x}}(k)\ v_{i,\mathrm{des}}^{\mathrm{y}}(k)\ \varphi_{i,\mathrm{des}}(k)\ \varphi_{i,\mathrm{des}}(k)\ e_{i,\mathrm{des}}^{\mathrm{p}}(k)\ l_{i,\mathrm{des}}(k)]^T \end{aligned} \tag{11}$$

where $v_{i,\mathrm{des}}^{\mathrm{x}}(k)$ is the desired speed of vehicle i.

$$\phi_i\big(X_i(k),U_i(k)\big)=\begin{bmatrix} u_i^{\mathrm{a}}(k)T_{\mathrm{s}}+v_i^{\mathrm{x}}(k) \\ \left(-v_i^{\mathrm{x}}(k)\dot{\varphi}_i(k)+\frac{1}{m_i}\left(-\frac{(C_i^{\mathrm{f}}+C_i^{\mathrm{r}})v_i^{\mathrm{y}}(k)}{v_i^{\mathrm{x}}(k)}-\frac{(C_i^{\mathrm{f}}a_i-C_i^{\mathrm{r}}b_i)\dot{\varphi}_i(k)}{v_i^{\mathrm{x}}(k)}+C_i^{\mathrm{f}}\delta_i(k)\right)\right)T_{\mathrm{s}}+v_i^{\mathrm{y}}(k) \\ \left(\frac{1}{I_i^z}\left(-\frac{(C_i^{\mathrm{f}}a_i-C_i^{\mathrm{r}}b_i)v_i^{\mathrm{y}}(k)}{v_i^{\mathrm{x}}(k)}-\frac{(C_i^{\mathrm{f}}a_i^2+C_i^{\mathrm{r}}b_i^2)\dot{\varphi}_i(k)}{v_i^{\mathrm{x}}(k)}+C_i^{\mathrm{f}}a_i\delta_i(k)\right)\right)T_{\mathrm{s}}+\dot{\varphi}_i(k) \\ \dot{\varphi}_i(k)T_{\mathrm{s}}+\varphi_i(k) \\ \big(v_0(k)-v_i(k)\big)T_{\mathrm{s}}+e_i^{\mathrm{p}}(k) \\ \big(v_i^{\mathrm{y}}(k)\cos\big(\varphi_i(k)-\theta_i^{\mathrm{r}}(k)\big)+v_i^{\mathrm{x}}(k)\sin\big(\varphi_i(k)-\theta_i^{\mathrm{r}}(k)\big)\big)T_{\mathrm{s}}+l_i(k) \end{bmatrix} \tag{9}$$

In the platoon, the desired speed of the follower vehicles should track the speed of the lead vehicle, thus let $v_{i,\mathrm{des}}^{\mathrm{x}}(k)=v_0(k)$. The desired lateral speed $v_{i,\mathrm{des}}^{\mathrm{y}}(k)=0$, but this does not mean that we expect the lateral speed to be exactly zero, as it is impossible for the vehicle's lateral speed to be zero when driving through a curve. We simply want the lateral speed to be as small as possible to reduce vehicle oscillation.

Assuming that the onboard equipment can measure the road radius R, meaning the road radius is known, then the ideal yaw rate is:

$$\dot{\varphi}_{i,\mathrm{des}}(k)=\frac{v_i^{\mathrm{x}}(k)}{R}. \tag{12}$$

The ideal yaw angle, as shown in Figure 3, is the angle between the tangent to the reference line at point p_i and the X-axis, i.e.,

$$\varphi_{i,\mathrm{des}}(k)=\theta_i^{\mathrm{r}}(k). \tag{13}$$

The ideal spacing error $e_{i,\mathrm{des}}^{\mathrm{p}}(k)=0$ and the ideal lateral distance error $l_{i,\mathrm{des}}(k)=0$, as we want to maintain a safe set distance between vehicles and ensure that each following vehicle travels along the reference line.

In the local problem for each following vehicle, define the same prediction horizon N_{p}. In the prediction horizon $[k,k+N_{\mathrm{p}}]$, three state trajectories are defined.

1) $X_i^{\mathrm{p}}(t|k)$: Predicted state trajectory.
2) $\tilde{X}_i(t|k)$: Assumed state trajectory.
3) $X_i^*(t|k)$: Optimal state trajectory.

Here, $t=0,1,\ldots,N_{\mathrm{p}}$. Similarly, define three control input trajectories.

1) $U_i^{\mathrm{p}}(t|k)$: Predicted control input trajectory.
2) $\tilde{U}_i(t|k)$: Assumed control input trajectory.
3) $U_i^*(t|k)$: Optimal control input trajectory.

Within the prediction horizon, define the reference state trajectory

$$\begin{aligned} &X_{i,\mathrm{des}}(t|k)= \\ &[v_{i,\mathrm{des}}^{\mathrm{x}}(t|k)\ v_{i,\mathrm{des}}^{\mathrm{y}}(t|k)\ \dot{\varphi}_{i,\mathrm{des}}(t|k)\ \varphi_{i,\mathrm{des}}(t|k) \\ &e_{i,\mathrm{des}}^{\mathrm{p}}(t|k)\ l_{i,\mathrm{des}}(t|k)]^T \end{aligned} \tag{14}$$

$$\begin{cases} v_{i,\mathrm{des}}^{\mathrm{x}}(t|k)=v_0(k) \\ v_{i,\mathrm{des}}^{\mathrm{y}}(t|k)=0 \\ \dot{\varphi}_{i,\mathrm{des}}(t|k)=\frac{\tilde{v}_i^{\mathrm{x}}(t|k)}{R} \\ \varphi_{i,\mathrm{des}}(t|k)=\theta_i^{\mathrm{r}}(t|k) \\ e_{i,\mathrm{des}}^{\mathrm{p}}(t|k)=0 \\ l_{i,\mathrm{des}}(t|k)=0 \end{cases} \quad t=0,1,...,N_p \tag{15}$$

where $\tilde{v}_i^{\mathrm{x}}(t|k)$ is the first term in the assumed state trajectory, and $\theta_i^{\mathrm{r}}(t|k)$ can be computed from the reference line information collected by the onboard equipment.

Now, we present the local optimization control problem for each vehicle i .

Problem $\mathcal{P}$: For each vehicle i, $i\in 1,2,\ldots,N$, at time k

$$\begin{aligned} \min_{U_i^{\mathrm{p}}(:|k)} &\sum_{t=0}^{N_{\mathrm{p}}-1} J_i\big(X_i^{\mathrm{p}}(t|k),y_i^{\mathrm{p}}(t|k),\tilde{y}_i(t|k),\tilde{y}_j(t|k),U_i^{\mathrm{p}}(t|k)\big) \\ &+\big\|X_i^{\mathrm{p}}(N_{\mathrm{p}}|k)-X_{i,\mathrm{des}}(N_{\mathrm{p}}|k)\big\|_{Q_i} \end{aligned} \tag{16a}$$

subject to

$$\begin{aligned} X_i^{\mathrm{p}}(t+1|k)&=\phi_i\big(X_i^{\mathrm{p}}(t|k),U_i^{\mathrm{p}}(t|k)\big) \\ y_i^{\mathrm{p}}(t|k)&=\gamma X_i^{\mathrm{p}}(t|k) \\ X_i^{\mathrm{p}}(0|k)&=X_i(k) \end{aligned} \tag{16b}$$

$$u_{i,\min}^{\mathrm{a}}\le u_i^{\mathrm{a,p}}(t|k)\le u_{i,\max}^{\mathrm{a}} \tag{16c}$$

$$\delta_{i,\min}\le\delta_i^{\mathrm{p}}(t|k)\le\delta_{i,\max} \tag{16d}$$

where

$$J_i\left(X_i^{\mathrm{p}}(t|k), y_i^{\mathrm{p}}(t|k), \tilde{y}_i(t|k), \tilde{y}_j(t|k), U_i^{\mathrm{p}}(t|k)\right) = \left\|X_i^{\mathrm{p}}(t|k) - X_{i,\mathrm{des}}(t|k)\right\|_{Q_i} + \left\|y_i^{\mathrm{p}}(t|k) - \tilde{y}_j(t|k)\right\|_{F_i} + \sum_{j\in\mathbb{N}_i} \left\|y_i^{\mathrm{p}}(t|k) - \tilde{y}_j(t|k)\right\|_{M_i} + \left\|U_i^{\mathrm{p}}(t|k)\right\|_{R_i} \tag{17}$$

where $U_i^{\mathrm{p}}(:|k) = [U_i^{\mathrm{p}}(0|k), \ldots, U_i^{\mathrm{p}}(N_{\mathrm{p}}-1|k)]$ represents the unknown control input trajectory to be optimized, $Q_i \in \mathbb{S}^2$, $F_i \in \mathbb{S}^2$, $M_i \in \mathbb{S}^2$, $R_i \in \mathbb{S}^2$ are the weighting matrices and they are all symmetric positive definite matrices. $\|o\|_{Q_i}$ represents $\|o\|_{Q_i} = o^{\mathrm{T}} Q_i o$. $\tilde{y}_i(t|k) = \gamma \tilde{X}_i(t|k)$ is the assumed output of the vehicle i, and $\tilde{y}_j(t|k) = \gamma \tilde{X}_j(t|k)$ is the assumed output of the neighboring vehicle j of the vehicle i. (16c) and (16d) represent constraints on the control inputs of acceleration and front wheel steering angle, ensuring that the vehicle's acceleration, deceleration, and front wheel steering angles remain within the physically feasible limits.

In the cost function (17)

1) $\left\|X_i^{\mathrm{p}}(t|k) - X_{i,\mathrm{des}}(t|k)\right\|_{Q_i}$ represents the penalty for the error between the predicted state trajectory of vehicle i and the desired state trajectory.

2) $\left\|y_i^{\mathrm{p}}(t|k) - \tilde{y}_j(t|k)\right\|_{F_i}$ represents the penalty for the error between the predicted output trajectory of vehicle i and the assumed output trajectory.

3) $\|y_i^{\mathrm{p}}(t|k) - \tilde{y}_j(t|k)\|_{M_i}$ represents the penalty for the error between the predicted output trajectory of vehicle i and the assumed output trajectory vehicle j.

4) $\left\|U_i^{\mathrm{p}}(t|k)\right\|_{R_i}$ represents the penalty for the control inputs of acceleration and front wheel steering angle for vehicle i .

Furthermore, $\left\|X_i^{\mathrm{p}}(N_{\mathrm{p}}|k) - X_{i,\mathrm{des}}(N_{\mathrm{p}}|k)\right\|_{Q_i}$ is the terminal cost function.

3.3 Algorithm of DMPC

The assumed control input trajectory $\tilde{U}_i(t|k)$ is iterated using the following equation

$$\tilde{U}_i(t|k) = \begin{cases} U_i^*(t+1|k-1), t = 0,1,\ldots,N_p-2 \\ U_i^*(N_{\mathrm{p}}-1|k-1), t = N_{\mathrm{p}}-1 \end{cases} \tag{18}$$

The assumed state trajectory $\tilde{X}_i(t|k)$ is then computed based on the assumed control input trajectory

$$\begin{aligned} \tilde{X}_i(t+1|k) &= \phi_i\left(\tilde{X}_i(t|k), \tilde{U}_i(t|k)\right) \\ \tilde{X}_i(0|k) &= X_i^*(1|k-1) \\ \tilde{y}_i(t|k) &= \gamma \tilde{X}_i(t|k) \\ t &= 0,1,\ldots,N_{\mathrm{p}}-1 \end{aligned} \tag{19}$$

The DMPC algorithm is presented as Algorithm 1:

Algorithm 1: DMPC Algorithm.

Initialization:
/* At time k =0, initialize the assumed state trajectory for vehicle $i = 1,2,\ldots,N$. */
Initialize the state variables $X_i(0)$ and control inputs $U_i(0)$ of vehicle i.
$\widetilde{U}_i(t|0) = U_i(0), t = 0,1,\ldots,N_p$;
for $t = 0$ *to* $N_p - 1$ **do**
  $\tilde{X}_i(t+1|0) = \phi_i\left(\tilde{X}_i(t|0), \tilde{U}_i(t|0)\right)$;
  $\tilde{y}_i(t|0) = \gamma \tilde{X}_i(t|0)$;
  $\tilde{X}_i(0|0) = X_i(0)$;
end
Iteration:
/* At time k>0, all vehicles $i = 1,2,\ldots,N$ perform iterative computations. */
while *the lead vehicle has not stopped* **do**
  1) Vehicle i gets the optimal control input trajectory $U_i^*(t|k)$ through solving the problem $\mathcal{P}$;
  2) Calculate the optimal state trajectory.
  for $t = 0$ *to* $N_p - 1$ **do**
    $X_i^*(t+1|k) = \phi_i(X_i^*(t|k), U_i^*(t|k))$;
    $X_i^*(0|k) = X_i(k)$;
  end
  3) Calculate the assumed control and output trajectories for the next time step using equations (18) and (19);
  4) Transmit $\tilde{y}_i(t|k+1)$ to vehicles $j \in \mathbb{O}_i$, receive $\tilde{y}_j(t|k+1)$ from vehicles $j \in \mathbb{N}i$, and obtain $Xi, \mathrm{des}(t|k+1)$ from the lead vehicle and onboard systems;
  5) Apply the first element of the optimal control input, $U_i(t) = U_i^*(0|k)$, to vehicle i;
  6) Set $k = k+1$;
end

Algorithm 1 presents the detailed steps of the DMPC algorithm. Within this framework, each vehicle in the fleet simultaneously solves its own optimization problem. This synchronized execution ensures the effectiveness of real-time control.

4 SIMULATION

The simulation will use CarSim 2016 and Matlab 2020b in conjunction. We validate the effectiveness of the longitudinal and lateral coupling platoon control model.

4.1 Parameter Settings

In this section, we will provide information about the vehicle and relevant parameters in the control algorithm. The vehicles in the simulation are homogeneous. The parameter settings can be found in Table 1 and Table 2.

Table 1: Vehicle parameters.

C_i^{f}	110000(N/rad)
C_i^{r}	110000(N/rad)
a_i	1.015(m)
b_i	1.950(m)
m_i	1412(kg)
I_i^z	1536.7(kg·m²)

Table 2: Control parameters.

N_{p}	6
Q_i	10^6 diag(5, 1, 5, 500, 10, 10)
F_i	10^6 diag(1, 100)
M_i	10^4 diag(1, 100)
R_i	diag(10, 10)
T_{s}	0.1(s)
$u_{i,\min}^{\mathrm{a}}$	-8(m/s²)
$u_{i,\max}^{\mathrm{a}}$	5(m/s²)
$\delta_{i,\min}$	-1(rad)
$\delta_{i,\max}$	1(rad)

4.2 Simulation Results

This case is used to verify the effectiveness of the longitudinal and lateral coupling platoon control model proposed in this paper.

Set the initial position of the lead vehicle $s_0 =$ 60m, the initial position of the following vehicle $s_1 =$ 45m, $s_2 = 30$m, $s_3 = 15$m, $s_4 = 0$m. Set the desired inter-vehicle distance as $d_{\mathrm{des}} = 15$m. The velocity trajectory of the lead vehicle is shown in Figure 5. The reference line is shown in Figure 6.

The simulation results are shown from Figures 7 to 10. Figure 7 presents the vehicle velocities. It can be observed that the following vehicles in the platoon closely track the lead vehicle's speed during constant, deceleration, and acceleration phases. Figure 8 shows the vehicle positions, demonstrating that safe distances between vehicles are maintained throughout the simulation, preventing collisions. Figure 9 illustrates the ideal inter-vehicle spacing errors. Under the PLF topology, since the first following vehicle only receives information from the lead vehicle, its reaction is more intense when the lead vehicle changes speed, resulting in relatively larger spacing errors. In

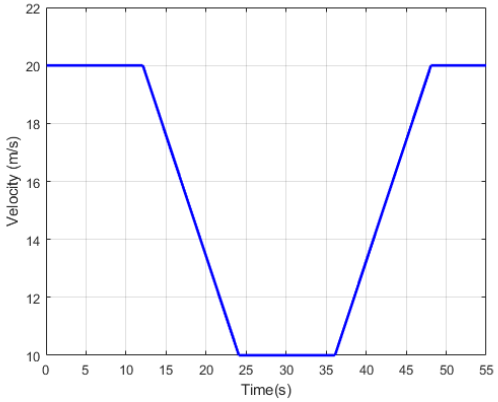

Figure 5: Lead vehicle's desired velocity trajectory.

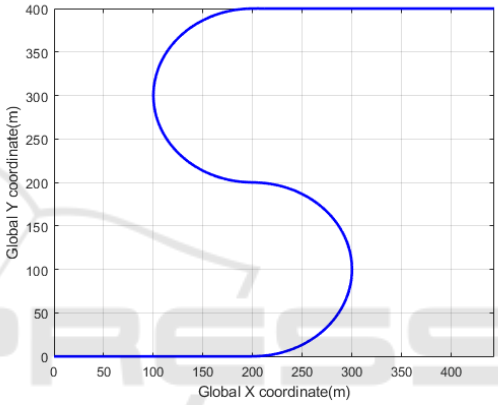

Figure 6: Reference line.

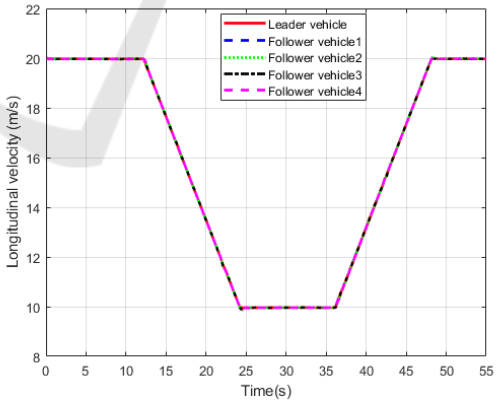

Figure 7: Velocity of vehicles.

contrast, the following vehicles can receive information from both the lead vehicle and the preceding vehicle, which leads to smaller spacing errors. Overall, the spacing errors between vehicles remain within a small range. Figure 10 illustrates the lateral distance error of the vehicles. It shows that the lateral distance error is minimal, indicating that the vehicles main-

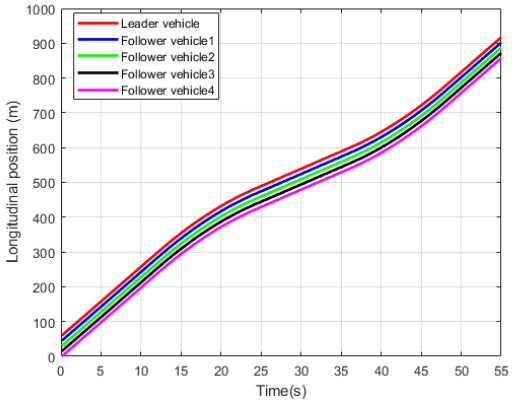

Figure 8: Longitudinal position of vehicles.

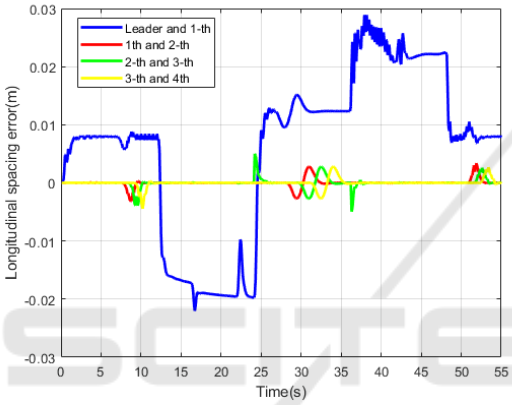

Figure 9: Longitudinal spacing error.

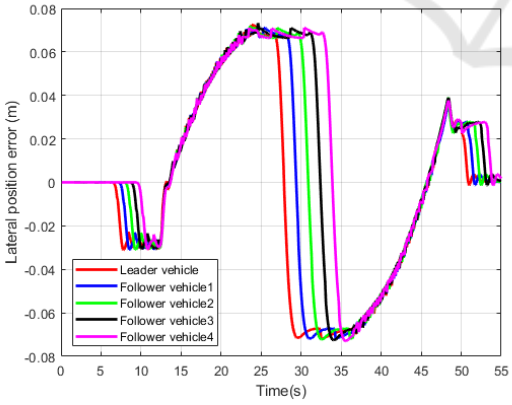

Figure 10: Lateral position error.

tain excellent lane-keeping performance while driving on roads with varying curvature, avoiding the cutting-corner problem and preventing drifting out of lane.

5 CONCLUSION

This paper focuses on platoon driving on curved roads by integrating a 3-DOF dynamic vehicle model with lateral distance in the Frenet coordinate system, forming a new longitudinal and lateral coupled platoon control model, which is controlled by DMPC (Distributed Model Predictive Control). Simulations demonstrate the good performance of the longitudinal-lateral coupled platoon control model. In the future, we plan to extend our research to cooperative control among more platoons, such as two or three platoons, and explore better models to improve control performance.

ACKNOWLEDGEMENTS

This work is supported by Zhejiang Provincial Natural Science Foundation of China (Grant No. LQ23F030014), National Natural Science Foundation of China (Grant No. 62303410), and Open Research Project of State Key Laboratory of Industrial Control Technology, Zhejiang University, China (Grant No. ICT2024B46).

REFERENCES

Basiri, M. H., Ghojogh, B., Azad, N. L., Fischmeister, S., Karray, F., and Crowley, M. (2020). Distributed nonlinear model predictive control and metric learning for heterogeneous vehicle platooning with cut-in/cut-out maneuvers. In *2020 59th IEEE Conference on Decision and Control (CDC)*, pages 2849–2856.

Bayuwindra, A., Ploeg, J., Lefeber, E., and Nijmeijer, H. (2020). Combined longitudinal and lateral control of car-like vehicle platooning with extended look-ahead. *IEEE Transactions on Control Systems Technology*, 28(3):790–803.

Dai, Y., Yang, Y., Wang, Z., and Luo, Y. (2022). Exploring the impact of damping on connected and autonomous vehicle platoon safety with cacc. *Physica A: Statistical Mechanics and its Applications*, 607:128181.

Dunbar, W. B. and Caveney, D. S. (2012). Distributed receding horizon control of vehicle platoons: Stability and string stability. *IEEE Transactions on Automatic Control*, 57(3):620–633.

Feng, Y., Yu, S., Sheng, E., Li, Y., Shi, S., Yu, J., and Chen, H. (2024). Distributed mpc of vehicle platoons considering longitudinal and lateral coupling. *IEEE Transactions on Intelligent Transportation Systems*, 25(3):2293–2310.

He, J., Zhao, F., Zhu, S., Li, S., and Xu, J. (2024). Priority-based deadlock recovery for distributed swarm obstacle avoidance in cluttered environments. In *2024*

IEEE/RSJ International Conference on Intelligent Robots and Systems (IROS), pages 14056–14062. IEEE.

Kianfar, R., Ali, M., Falcone, P., and Fredriksson, J. (2014). Combined longitudinal and lateral control design for string stable vehicle platooning within a designated lane. In *17th International IEEE Conference on Intelligent Transportation Systems (ITSC)*, pages 1003–1008.

Kwon, J.-W. and Chwa, D. (2014). Adaptive bidirectional platoon control using a coupled sliding mode control method. *IEEE Transactions on Intelligent Transportation Systems*, 15(5):2040–2048.

Li, S. E., Zheng, Y., Li, K., Wu, Y., Hedrick, J. K., Gao, F., and Zhang, H. (2017). Dynamical modeling and distributed control of connected and automated vehicles: Challenges and opportunities. *IEEE Intelligent Transportation Systems Magazine*, 9(3):46–58.

Ma, K., Wang, H., and Ruan, T. (2021). Analysis of road capacity and pollutant emissions: Impacts of connected and automated vehicle platoons on traffic flow. *Physica A: Statistical Mechanics and its Applications*, 583:126301.

Negenborn, R. and Maestre, J. (2014). Distributed model predictive control: An overview and roadmap of future research opportunities. *IEEE Control Systems Magazine*, 34(4):87–97.

Rajamani, R., Tan, H.-S., Law, B. K., and Zhang, W.-B. (2000). Demonstration of integrated longitudinal and lateral control for the operation of automated vehicles in platoons. *IEEE Transactions on Control Systems Technology*, 8(4):695–708.

Wei, S., Zou, Y., Zhang, X., Zhang, T., and Li, X. (2019). An integrated longitudinal and lateral vehicle following control system with radar and vehicle-to-vehicle communication. *IEEE Transactions on Vehicular Technology*, 68(2):1116–1127.

Wu, J., Wang, Y., and Yin, C. (2022). Curvilinear multilane merging and platooning with bounded control in curved road coordinates. *IEEE Transactions on Vehicular Technology*, 71(2):1237–1252.

Zeng, J., Qian, Y., Li, J., Zhang, Y., and Xu, D. (2023). Congestion and energy consumption of heterogeneous traffic flow mixed with intelligent connected vehicles and platoons. *Physica A: Statistical Mechanics and its Applications*, 609:128331.

Zhao, H., Sun, D., Zhao, M., Pu, Q., and Tang, C. (2022). Combined longitudinal and lateral control for heterogeneous nodes in mixed vehicle platoon under v2i communication. *IEEE Transactions on Intelligent Transportation Systems*, 23(7):6751–6765.

Zheng, Y., Li, S. E., Li, K., Borrelli, F., and Hedrick, J. K. (2017). Distributed model predictive control for heterogeneous vehicle platoons under unidirectional topologies. *IEEE Transactions on Control Systems Technology*, 25(3):899–910.

Zuo, Z., Yang, K., Wang, H., Wang, Y., and Wu, Y. (2024). Distributed mpc for automated vehicle platoon: A path-coupled extended look-ahead approach. *IEEE Transactions on Intelligent Vehicles*, pages 1–13.